Ultrafast TSPD on the basis of CeB_6 sensor

A A Kuzanyan, A S Kuzanyan and V R Nikoghosyan

Institute for Physical Research, Ashtarak-2, 0203, Republic of Armenia

E-mail: astghik.kuzanyan@gmail.com

Abstract. The results of computer simulation of heat distribution on the sensor of Thermoelectric Single Photon Detector after photon absorption are presented in this work. The kinetic processes emerging after the absorption of 100 eV (hard UV) and 1 KeV (X-ray) energy photons in different areas of the absorber for different sensor and absorber geometries are investigated. The calculations were performed for the tungsten absorber and the cerium hexaboride sensor. It is shown, that waveform of time dependence of response doesn't strongly depend from the depth of photon thermalization area in absorber and the height on which the temperature gradient on the edges of thermoelectric sensor is measured.

1. Introduction

The past 15 years has seen a dramatic increase in interest in new detection technologies because single-photon detectors are one of the most important components in the fields of quantum information and communications technology. In addition to quantum information and quantum cryptography, single-photon detectors are required in researches in the fields of space astronomy, single-molecule spectroscopy, high energy physics, measuring systems for applications in medicine, homeland security, DNA sequencing, elemental microanalysis, traditional and quantum-enabled metrology, analysis of defects in microchips, positron emission tomography etc. [1]. Superconducting nanowire single photon detectors (SNSPD) outperform other single photon detector technologies on several merits such as quantum efficiency, timing jitter, dark count rates, and broad spectral sensitivity [2]. SNSPD offers single-photon sensitivity from visible to mid-infrared wavelengths operating at cryogenic temperatures well below the critical temperature of the device [3, 4]. The thermoelectric single-photon detector (TSPD) is one of the real competitors to SNSPD [5, 6]. The TSPD operation principle is based on photon absorption by absorber as a result of which a temperature gradient is generated on the edges of the thermoelectric sensor. Materials which can be used to prepare absorber and sensor, the achievable count rates and energy resolution are given in publications [7-9]. The conception of TSPD using nanoscale sensor is proposed in [10, 11].

The results of computer modeling of heat distribution processes after absorption of 0.1-1 keV energy photons in different parts of the W absorber for different geometries of absorbers and $(La, Ce)B_6$ thermoelectric sensors are presented in [11]. The results of calculations show that the temperature gradient decline time is less than the time of heat passage through the Kapitza contact for all used sensor geometries, and it is realistic to detect photons about 0.1-1 keV and determine their energy with accuracy of not less than 1%. High count rates up to 200 GHz can be achieved. The results of computer simulation of heat distribution processes in cerium hexaboride (CeB_6) sensor of TSPD after single photon absorption on the different areas of the surface of the tungsten (W) absorber are presented in [10, 12]. In this work we have studied more subtle effects. The results of computer modeling of the processes of heat distribution after photons' absorption on absorber surface, at the half

of the absorber thickness and at the absorber-substrate boundary are presented. The temperature difference at the ends of the CeB_6 sensor was also registered at different heights.

2. Detection pixel of TSPD

The sensor of the thermoelectric detector consists of three parts – the absorber, the heat sink and the connecting bridge made of thermoelectric material. The scheme of the TSPD sensitive element is given in figure 1. Such a sensor does not require either a separate power unit or a bias voltage. Therefore, it does not need additional leads for electronic circuitry. A matrix detector built on them will have very simple engineering and electronic structure. In this work, as earlier in [12], the sensitive element consisting of CeB_6 thermoelectric and W absorber will be considered. The figure also shows the directions of the coordinate axes: x is parallel to the axis of symmetry of the sensor (corresponding to the length of geometric shapes), y is perpendicular to the x (width), z is perpendicular to x, y and the substrate surface (height). The onset of coordinates is located at the corner of the absorber, on the substrate-absorber boundary. Such consideration will enable us to determine uniquely the coordinates of the center of thermalization zone of the photon and the height at which the temperature gradient between the ends of the thermoelectric bridge is measured.

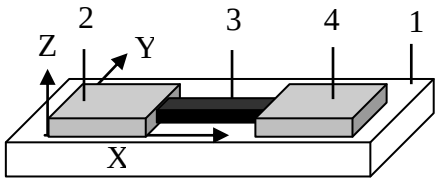

Figure 1. Detection pixel of TSPD: 1 – substrate, 2 – absorber, 3 – thermoelectric bridge, 4 – heat sink.

As is shown in [12], photons with 100 eV energy are absorbed with 100 % probability in 0.5 μm thick tungsten. And this value of thickness of absorbers and of the thermoelectric bridge is used in calculations in the case of absorption of 100 eV energy photon. For 1 keV the thickness is 1.5 μm.

3. Computing technique

The calculations were based on the heat conduction equation and were carried out by the matrix method for differential equations. The operating temperature of the detector was taken equal to 9 K, in which CeB_6 has the highest figure of merit. The modeling of thermal processes occurring in the absorption of a photon is as follows. The entire volume of the absorber and the bridge was splitted into cells of Δx, Δy and Δz sizes. These dimensions were typically of the order of 0.1 μm. Obviously, the greater the number of cells will provide for more accurate calculations, but more time consuming.

The thermal processes were modeled according to the following algorithm.

- For all cells the initial temperature was set at 9 K.
- The cell where the photon is absorbed was chosen in the absorber.
- According to the formula $\Delta T = E/V\rho c$, where E is the energy of the absorbed photon, ρ is the density, V is the cell volume and c is the specific heat capacity, the initial temperature of the cell $T_0 = 9\ \mathrm{K} + \Delta T$ was calculated.
- The temperature of all cells for each time point t_n was determined.

The thermal processes modeling in details is presented in [10].

4. Results

The results of calculations of the time dependence of temperature distribution in the sensor of the thermoelectric detector after absorption of 100 eV and 1 keV energy photons are presented in table 1. We considered photon absorption at different heights in the central part of the absorber. The calculations are performed for the cases when temperature gradient emerging on the thermoelectric is measured at different heights. Table 1 shows the calculation numbers, z coordinate of center of thermalization area – (Z_1), z coordinate of the level at which temperature difference ΔT at the ends of

the bridge is measured – (Z_2), maximum ΔT value derived from computer simulation – (ΔT_{max}), the time when this maximum is reached – (t_m), the voltage difference at the ends of the bridge – (ΔU_{max}) = $\Delta T_{max} S$ (calculated using the value of Seebeck coefficient S = 150 μV/K averaged from literature reports), the time of the gradient fall to the background value ΔT_{max} /10 – (t_b) and the count rate of the detector – (R) = $1/t_b$.

The following (x×y×z) sensor geometry is used. For the calculation of 100 eV energy photon absorption the sizes of absorbers and thermoelectric bridge are 5×0.5×0.5 μm^3 and 0.01×0.5×0.5 μm^3 respectively. For 1 keV photon absorption we use 5×0.5×1.5 μm^3 absorbers and 0.01×0.5×1.5 μm^3 thermoelectric bridge. Calculations 1-4 (shown in table by Italic) correspond to 100 eV energy photon absorption; calculations 5-13 are for 1 keV energy photons.

Table 1. Calculations and detector parameters for photons absorption processes.

No	Z_1, μm	Z_2, μm	ΔT_{max}, 10^{-4} K	ΔU_{max}, μV	t_m, ps	t_b, ps	R, GHz
1	*0.4*	*0.5*	*21.1*	*0.316*	*3.6*	*101.1*	*9.9*
2	*0.4*	*0.1*	*21*	*0.315*	*3.9*	*101.1*	*9.9*
3	*0.1*	*0.5*	*21*	*0.315*	*3.9*	*101.1*	*9.9*
4	*0.1*	*0.1*	*21*	*0.315*	*3.9*	*101.1*	*9.9*
5	1.2	1.5	75.5	1.13	1.8	57	17.5
6	1.2	0.1	74.9	1.124	2.4	57.6	17
7	1.2	0.7	75.2	1.128	2.1	57	17.5
8	0.3	1.5	75.1	1.127	2.1	57	17.5
9	0.7	1.5	75.3	1.13	2.1	57	17.5
10	0.3	0.1	74.6	1.119	2.7	57.6	17
11	0.7	0.1	74.7	1.121	2.4	57.6	17
12	0.3	0.7	74.9	1.124	2.4	57.6	17
13	0.7	0.7	75	1.125	2.4	57.3	17

4.1. Registration of photons with 100 eV energy

The equation of heat distribution from a limited volume in the three-dimensional model was solved for various Z_1 and Z_2 parameters. In figure 2 the results of calculation of time dependence of temperature difference appearing across the thermoelectric bridge are given for 100 eV energy photon absorption. The $\Delta T(t)$ curves are almost identical for calculations 1 (the photon is absorbed at the surface of the absorber and $\Delta T(t)$ is measured on the surface of thermoelectric), 2 (photon is absorbed at the surface of the absorber and $\Delta T(t)$ is measured on the thermoelectric-substrate boundary), 3 (photon is absorbed on the thermoelectric-substrate boundary and ΔT is measured on the surface of thermoelectric) and 4 (photon is absorbed on thermoelectric-substrate boundary and ΔT is measured on thermoelectric-substrate boundary). As can be seen from the inset of figure 2, the curves differ only for the first 3 ps from the start of the process. The curves are practically identical after achievement of the maximum. As a result, we have the same values of ΔT_{max}, ΔU_{max} and R parameters of the detector for the calculations shown in table 1. The maximum difference between the curves is achieved at t = 0.9 ps, and reaches 1.8×10^{-4} K. This value is lower than the background value, which for 1-4 calculations is 2.1×10^{-4} K.

Summarizing the data in table 1 and figure 2, we can conclude that for 100 eV energy photon absorption the generated signal emerging on the thermoelectric bridge does not depend from on the depth at which the photon is thermalised and the height at which the signal is registered.

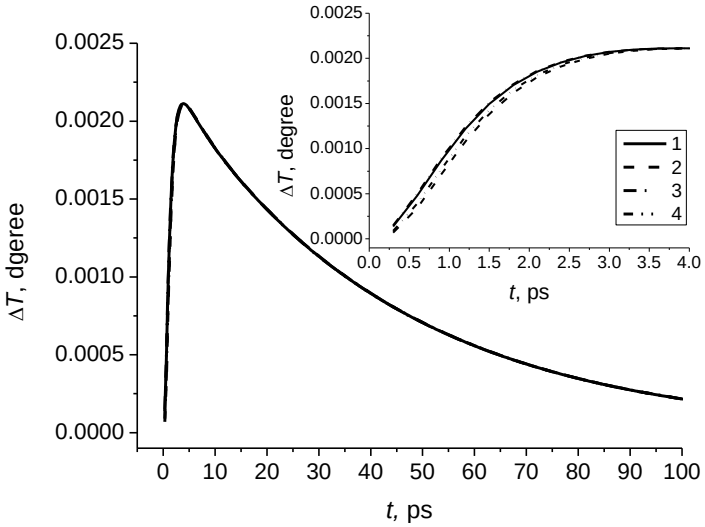

Figure 2.$\Delta T(t)$ dependence for case of tungsten absorber of $5\times0.5\times0.5$ μm^3 size, CeB_6 sensor - $0.01\times0.5\times0.5$ μm^3, 100 eV photon absorption.

4.2. Registration of photons with 1keV energy

The calculations for 1 keV energy photon absorption are done for three positions of the thermalization area: near the surface (the calculations 5-7), on the half-height of the absorber (the calculations 9, 11, 13) and near the boundary of the absorber-substrate (8, 10, 12).Three values of the parameter Z_2 were also used: the surface of the sensor (the calculations 5, 8, 9), the half-height (the calculations 7, 12, 13) and the absorber-substrate boundary (the calculations 6, 10, 11). The calculation results for 1 keV photon absorption on the half-height of the absorber are shown in figure 3.

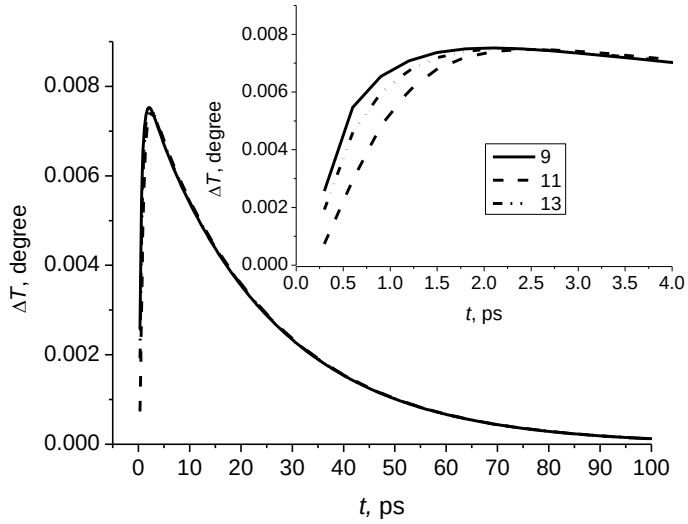

Figure 3. $\Delta T(t)$ dependence for case of W absorber with the size of $5\times0.5\times1.5$ μm^3, CeB_6 sensor – $0.01\times0.5\times1.5$ μm^3, 1 keV photon, parameters Z_1 = 0.7 μm; Z_2 – 1.5 μm, (calculation 9), 0.1 μm (11) and 0.7 μm (13).

As can be seen, in this case as well, the shape of the curves significantly differs only in the beginning of the process of heat propagation from the photon thermalization zone. After reaching the maximum of $\Delta T(t)$ the curves practically merge.

The results of other calculations corresponding to the photon absorption on the absorber-substrate boundary and at the surface of the absorber are shown in figure 4.

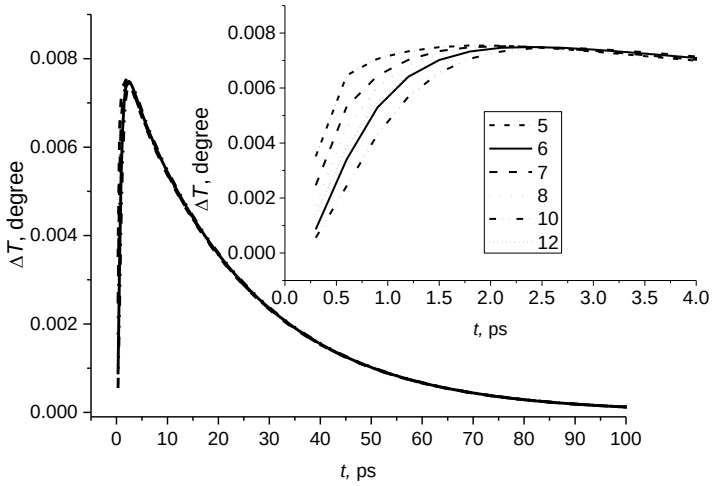

Figure 4. $\Delta T(t)$ dependence for case of W absorber with the size of $5\times0.5\times1.5$ μm^3, CeB_6 sensor – $0.01\times0.5\times1.5$ μm^3, 1 keV photon, parameter Z_1 – 0.3 μm (calculation 8, 10, 12), and 1.2 μm (calculation 5, 6, 7).

The insert of figure 4 clearly shows that at the beginning of the process the difference between the curves' shapes is quite big. The maximum difference is between the curves 5 and 10 which reaches 2.8×10^{-3} K at $t = 0.9$ ps. However, if $t > 2$ ps, the curves merge the detector characteristics for these calculations are almost identical (table 1).

5. Conclusions

According to results of computer modeling presented in this paper it can be concluded that the energy of the absorbed photon can be determined by using maximum value of the obtained signals irrespective to the photon absorption point. This is an additional advantage showing that TSPD can really compete with superconducting detectors.

Acknowledgements

This work was supported by the RA MES State Committee of Science and Russian Foundation for Basic Research (RF) in the frames of the joint research projects SCS 15RF-018 and RFBR 15-53-05047 accordingly.

References

1. Eisaman M D, Fan J, Migdall A and Polyakov S V 2011 *Rev. Sci. Instrum.* **82** 071101
2. Hadfield R H2009 *Nat. Phot*. **3** 696
3. Atikian H A, Eftekharian A, Jafari Salim A, Burek M J, Choy J T, Hamed Majedi A and Lonar M 2014 *Appl. Phys. Lett.* **104** 122602
4. Liu D, Miki S, Yamashita T, You L, Wang Z and Terai H 2014 *Optics Express* **22** 21167
5. Van Vechten D, Wood K, Fritz G, Horwitz J, Gyulamiryan A, Kuzanyan A, Vartanyan V and Gulian A 2000 *NIMA* **444** 42
6. Gulian A, Wood K, Van Vechten D and Fritzdet G 2004 *J. Mod. Opt.* **51** 1467
7. PetrosyanV A 2011 *J. Contemp. Phys. (Arm. Acad. Sci.)* **46** 125
8. Kuzanyan A A, Petrosyan V A and Kuzanyan A S 2012 *JPCS* **350** 012028
9. Kuzanyan A A and Kuzanyan A S 2013 *Proc. SPIE* **8773** 87730L
10. Kuzanyan A A 2014 *Nano Studies* **9** 93-102
11. Kuzanyan A S, Nikoghosyan V R and Kuzanyan A A 2015 *Proc. SPIE* **9504** 95040O
12. Kuzanian A, Nikoghosyan V and Kuzanyan A 2015 *Sensors & Transducers* **191** (8)57